NACA RM A54H26a

RESEARCH MEMORANDUM

THE APPLICATION OF A SIMPLIFIED LIFTING-SURFACE THEORY

TO THE PREDICTION OF THE ROLLING EFFECTIVENESS OF

PLAIN SPOILER AILERONS AT SUBSONIC SPEEDS

By Ralph W. Franks

Ames Aeronautical Laboratory
Moffett Field, Calif.

NATIONAL ADVISORY COMMITTEE
FOR AERONAUTICS
WASHINGTON
December 6, 1954

iQ

UNCLASSIFIED

NATIONAL ADVISORY COMMITTEE FOR AERONAUTICS

RESEARCH MEMORANDUM

THE APPLICATION OF A SIMPLIFIED LIFTING-SURFACE THEORY

TO THE PREDICTION OF THE ROLLING EFFECTIVENESS OF

PLAIN SPOILER AILERONS AT SUBSONIC SPEEDS

By Ralph W. Franks

SUMMARY

A method is described for predicting the subsonic rolling effective-
ness at zero angle of attack for plain spoiler ailerons. The spoilers
considered were of constant-percent-chord height and mounted normal to
the wing surface along the 70-percent-chord line. An extension of the
method to include additional types of spoiler ailerons appears possible.
A simplified lifting-surface theory developed for flap-type ailerons is
used together with two-dimensional-spoiler data and an empirical correc-
tion for the effective spanwise location on swept wings. A comparison
is made of the predicted rolling moments with experimentally obtained
values for a series of models, and the agreement is shown to be good.

INTRODUCTION

As a result of the current interest in the application of retractable
spoiler ailerons as lateral controls on high-speed aircraft, a considerable
number of tests have been made using various types of spoiler configura-
tions. The results of some of these tests are presented in references 1
to 10, and reference 11 contains a bibliography of spoiler information.

The great number of wing-plan-form-spoiler combinations possible,
however, creates a need for a method of predicting spoiler rolling-moment
effectiveness which accounts for as many of the variables involved as
possible. In references 7 and 9 are presented the results of two attempts
to predict spoiler effectiveness. Each of these methods is based on the
application of a flap-effectiveness theory. The agreement of experimental
and predicted results is good for unswept wings. For a swept wing, how-
ever, the method of reference 9 is inapplicable since the method was
developed using the antisymmetrical span loading of unswept wings only.

Reference 7 described an empirical modification to this method to account for the effects of sweep; however, a comparison of the predicted and experimental spoiler effectiveness shows the predicted values to be too high for spoilers on swept wings.

It is the purpose of this report to describe a method of predicting spoiler rolling-moment effectiveness based on the simplified lifting-surface flap theory of reference 12. To apply this flap theory to spoilers, it was necessary to obtain test data of spoilers on two-dimensional wings, and to employ an empirical correction when predicting the effectiveness of partial-span spoilers on swept wings. The results of applying the present method to the configurations described in references 1 to 8 (see table I and fig. 1) and the comparison with the experimental data are presented herein.

NOTATION

The coefficients and symbols used in this report are defined as follows:

A   wing aspect ratio

b   wing span, measured perpendicular to plane of symmetry, ft

C_l rolling-moment coefficient, $\dfrac{\text{rolling moment}}{qSb}$

$C_{l_{ex}}$ rolling moment obtained experimentally

C_{l_t} rolling moment predicted by application of theory

C_{l_δ} rolling moment due to aileron deflection, $\dfrac{\partial C_l}{\partial \delta}$ (from ref. 12), per radian

c   wing chord (measured parallel to plane of symmetry), ft

H   height of spoiler above wing section mean line, measured normal to mean line, ft

h   height of spoiler above wing surface, measured normal to wing surface, ft

M   Mach number

q   free-stream dynamic pressure, lb/sq ft

R   Reynolds number, based on the mean aerodynamic chord

S	wing area, sq ft
t	maximum airfoil section thickness, ft
x_s	distance from wing leading edge to spoiler, measured parallel to plane of symmetry, ft
y_s	distance from model center line to edge of spoiler, measured perpendicular to plane of symmetry, ft
z_s	ordinate of airfoil section at spoiler location, ft
α	angle of attack of the wing-chord plane with reference to free stream, deg
Δ	prefix denoting an increment
$\Delta\alpha_s$	effective change in angle of attack due to deflection of spoiler, measured at $C_L = 0$, radians
δ	angle of deflection of full wing-chord control surface (from ref. 12), radians
η	dimensionless lateral coordinate, $\dfrac{y_s}{b/2}$
η_i	spanwise location of inboard end of spoiler, $\dfrac{y_{s_{inboard}}}{b/2}$
η_o	spanwise location of outboard end of spoiler, $\dfrac{y_{s_{outboard}}}{b/2}$
θ	angle used in determining empirical correction factor, deg
Λ	angle of sweepback, deg (Subscripts denote line referred to: c/4, quarter chord; s, spoiler; t, trailing edge.)
λ	wing taper ratio

DEVELOPMENT OF METHOD

The spoiler configuration chosen for analysis was a plain spoiler aileron located on the wing upper surface along the 70-percent-chord line and of constant-percent-chord height. This configuration was selected because more experimental data were available for this type than for any other single type.

The procedure used in obtaining theoretical values of the spoiler rolling effectiveness was similar to that used in references 7 and 9. Values of C_{l_δ} obtained from a flap theory were multiplied by a value of $\Delta\alpha_s$, representing the effective change in section angle of attack due to spoiler deflection, to give the predicted rolling-moment coefficient. For the present investigation, however, reference 12 was used to obtain values of C_{l_δ} because this theory was developed for use with antisymmetrical control deflections on wings of arbitrary plan forms, and it has given good results with flap-type controls.

The values of $\Delta\alpha_s$ used were obtained by testing a series of symmetrical airfoil sections ranging in thickness from 6.0- to 16.3-percent chord and measuring the change in angle of attack for zero lift caused by spoilers of various heights and chordwise locations on the airfoil. The tests were made in a 2- by 5-foot two-dimensional wind tunnel at a Reynolds number of 2 million. Plotting of these values of $\Delta\alpha_s$ against H/c resulted in a single curve for each chordwise location of the spoilers. The curves are reproduced in figure 2. Some data for trailing-edge spoilers are given in reference 10.

A comparison of the rolling-moment coefficient predicted as described above with experimentally obtained values showed that while the characteristics with full semispan spoilers on swept wings and both full- and partial-semispan spoilers on straight wings could be predicted with good accuracy, the predictions with partial-semispan spoilers on swept wings were not acceptably accurate. It was suspected that the inaccuracies in the prediction for partial-semispan spoilers on swept wings were caused by the spanwise flow of the spoiler wake in an outboard direction as described in reference 8.

In order to account for the effect of this spanwise flow of the wake on the effectiveness of spoilers on swept wings, an empirical correction was developed. The experimental values of C_l for models 1, 2, 3, and 12 (described in table I and fig. 1) having spoilers of 10-percent-chord height, mounted along the 70-percent-chord line, and extending inboard from the wing tip to various values of η_i were compared with the theoretical values of C_l obtained by application of the flap theory of reference 12 as described above. The values of η_i effective, which would yield a theoretical C_l equivalent to the experimental were then determined and laid off on the wing trailing edge as shown in figure 3. The average angle, θ, obtained for each wing studied was then determined, and its variation with sweep of the spoiler is shown in figure 4. Limited data indicated that these values of θ could be used for spoilers extending outboard from the wing center line. The correction was applied as shown in figure 5 to the remainder of the spoiler configurations tested on models 1, 2, 3, and 12, and also to the spoiler configurations tested on the remainder of the models listed in table I.

For models 9 and 12, the calculations of C_{l_δ} included the compressibility corrections of the theory of reference 12.

APPLICATION OF METHOD

The procedure in obtaining a value of C_l for a particular wing-spoiler configuration consists of first determining a value for the effective location of the inboard end of the spoiler, $\eta_{i_{effective}}$, and for the effective location of the outboard end of the spoiler, $\eta_{o_{effective}}$. Using these values to locate the effective spoiler location, the C_{l_δ} is obtained from reference 12.

In determining $\eta_{effective}$, $\Delta\eta$, which is the difference between the actual end of the spoiler and the effective location, is computed as shown in figure 5. Adding $\Delta\eta$ to η gives $\eta_{effective}$; however, if $\eta_{o_{effective}}$ exceeds 1.0, as would be the case for the spoiler extending almost to the wing tip on a highly swept wing, the C_{l_δ} corresponding to $\eta_o = 1$ should be used.

The values of C_{l_δ} for full chord flaps obtained from reference 12 can be used in conjunction with $\Delta\alpha_s$ to obtain C_l since $\Delta\alpha_s$ is equivalent to δ. In the present report, it is considered that a spoiler is deflected on one wing panel only, and therefore one half the value of C_{l_δ} given in reference 12 should be used since the values therein are for two controls antisymmetrically deflected.

To illustrate the application of the method, a sample calculation is outlined below.

Assumed wing characteristics:

$$A = 4$$

$$\lambda = 0.62$$

$$\Lambda_{c/4} = 40.18^\circ$$

Airfoil section, NACA 64A010 (streamwise)

Assumed spoiler characteristics:

$$\eta_i = 0.15 \ b/2$$

$$\eta_o = 0.60 \ b/2$$

$$h/c = 0.08$$

$$x_s/c = 0.70$$

Calculations:

The airfoil section ordinate at 70-percent chord is 3.127-percent chord; therefore, $H/c = h/c + 0.0313 = 0.1113$. From figure 2, $\Delta\alpha_s = 0.128$. Applying equation (26) of reference 12,

$$\tan \Lambda_s = \tan \Lambda_{c/4} - \frac{4\left[0.75 - (1 - \frac{x_s}{c})\right]}{A}\left(\frac{1 - \lambda}{1 + \lambda}\right)$$

$$= 0.75064$$

$$\Lambda_s = 36.89^{\circ}$$

$$\tan \Lambda_t = \tan \Lambda_{c/4} - \frac{4(0.75)}{A}\left(\frac{1 - \lambda}{1 + \lambda}\right) = 0.66854$$

$$\Lambda_t = 33.76^{\circ}$$

From figure 5:

$$\Delta\eta_i = \frac{4(1 - 0.70)}{4(1.62)}\left[1 - (0.38)(0.15)\right]\frac{\cos 33.8^{\circ} \sin 30.5^{\circ}}{\cos 64.3^{\circ}}$$

$$\Delta\eta_i = 0.170$$

$$\Delta\eta_o = \frac{4(1 - 0.70)}{4(1.62)}\left[1 - (0.38)(0.60)\right]\frac{\cos 33.8^{\circ} \sin 30.5^{\circ}}{\cos 64.3^{\circ}}$$

$$\Delta\eta_o = 0.139$$

$$\eta_{i_{effective}} = \eta_i + \Delta\eta_i = 0.15 + 0.170 = 0.320$$

$$\eta_{o_{effective}} = \eta_o + \Delta\eta_o = 0.60 + 0.139 = 0.739$$

UNCLASSIFIED

Assuming C_l is desired at a low enough Mach number so that $\sqrt{1 - M^2} \approx 1.0$, the following value of C_{l_δ} is obtained from reference 12: at $\eta_{i_{effective}}$ $C_{l_\delta} = 0.080$ and at $\eta_{o_{effective}}$ $C_{l_\delta} = 0.369$

$$C_{l_\delta} = 0.289$$

Since this example involves a spoiler deflected on one wing panel only, this value is halved

$$C_{l_\delta} = 0.289/2 \approx 0.145$$

Using the value of $\Delta\alpha_s$ obtained above:

$$C_l = (0.145)(0.128) = 0.019$$

DISCUSSION

In order to evaluate the results obtained by the application of the method described above, the predicted rolling-moment coefficients at zero angle of attack for a number of models having various wing-spoiler configurations were plotted against the rolling-moment coefficients obtained experimentally from references 1 through 8. These plots are presented in figures 6 to 19. In most cases the agreement is good, and no systematic variation has been found for differences between predicted and experimental values; however, in many cases the increment of $C_{l_{ex}}$ obtained by the addition of a spoiler segment from $\eta = 0.80$ to $\eta = 1.00$ to a spoiler extending outboard from the fuselage (or wing center line) was greater than would be predicted.

In computing the values of C_{l_δ} used to obtain the theoretical rolling-moment coefficients the effects of compressibility were taken into account according to the method discussed in reference 12. The effect of applying this procedure is shown in figure 15 where rolling-moment data taken at three Mach numbers are presented. While the predicted values of C_l are about 10 percent lower than the experimental values reported in reference 6, the effects of compressibility seem to be adequately accounted for by the method.

Although the bulk of the available data are for spoilers mounted along the 70-percent-chord line, figure 8 shows the results of applying the method to spoilers along the 60- and 80-percent-chord lines on model 2. The effective spoiler spanwise location was determined using θ obtained from figure 4 and calculated according to the equations shown in figure 5. The agreement of predicted and experimental results was essentially the same for this range of spoiler chordwise locations.

In the development of the method, as described above, it was found necessary to correct for the spanwise flow of the wake behind the spoiler on sweptback wings by an empirical correction. It is of interest that the data of reference 8 indicate that the computed effective spanwise location of the inboard end of the spoiler on this model coincided with the point at which the separated area behind the spoiler on the upper surface reached the trailing edge of the wing at zero angle of attack. At this point the spanwise loading indicated a decrement of lift due to spoiler action. At the outboard end of the spoiler the flow behind the spoiler was separated to the wing tip as would also be predicted by the computed spanwise correction.

In the present method, the rolling-moment coefficient is predicted only for zero angle of attack. While two-dimensional spoiler data gave no indication that spoiler effectiveness would vary with angle of attack for angles less than those at which separation begins ahead of the spoiler, the three-dimensional wings generally exhibited an increase of rolling moment with angle of attack at low angles. Figure 20 shows typical variations for four of the models considered in this report. The large effect of a change of airfoil section on model 2 should be noted. (The airfoil sections used are described in detail in reference 1, and consisted of a thin symmetrical section which was modified by the addition of a drooped leading edge of increased radius. Both sections were identical aft of 40-percent chord.) This large variation is in contrast with the negligible differences in rolling moments produced at zero angle of attack for a given spoiler configuration on each of the two wings. Because of the many variables involved, generalized curves of the variation of C_l with angle of attack for various wing-spoiler combinations have not been developed, and the curves of figure 20 should not be used as such. Since this increase of C_l with angle of attack occurs for almost all configurations studied, the predicted value of C_l at zero angle of attack can be considered to be conservative up to the angle of attack at which separation begins on the wing without a deflected spoiler.

The range of plan forms considered by the theory of reference 12 included any arbitrary plan form having a straight quarter-chord line across the semispan. While both straight and sweptback wings having a variety of taper ratios were studied in the present report, no data exist for spoilers on sweptforward wings.

The method as described above was developed for a particular type of spoiler aileron; however, it is believed that the method can be extended to other types of spoilers if values of $\Delta\alpha_s$ and $\Delta\eta$ can be determined. While only spoilers of constant-percent-chord height were studied in this report, it is believed that spoilers of constant height could be dealt with as is done with constant-chord flap-type controls in reference 12.

CONCLUDING REMARKS   UNCLASSIFIED

The low-speed rolling-moment coefficient produced at zero angle of attack by plain spoilers of constant-percent-chord height and located on the wing upper surface along the 70-percent-chord line can be predicted by a method based on the simplified lifting-surface theory of reference 12.

Agreement between experimentally obtained values of the rolling-moment coefficient and those predicted by this method is shown to be good.

Although the type of spoiler investigated was that for which the most data are presently available, it is believed that the method can be extended to apply to other types of spoiler ailerons.

Ames Aeronautical Laboratory
    National Advisory Committee for Aeronautics
        Moffett Field, Calif., Aug. 26, 1954

REFERENCES

1. Franks, Ralph W.: Tests in the Ames 40- by 80-Foot Wind Tunnel of the Aerodynamic Characteristics of Four Airplane Models With Plain Spoiler Ailerons. NACA RM A54H26, 1954.

2. Bollech, Thomas V., and Pratt, George L.: Effects of Plain and Step Spoiler Location and Projection on the Lateral Control Character-istics of a Plain and Flapped 42° Sweptback Wing at a Reynolds Number of 6.8×10^6. NACA RM L9I20a, 1950.

3. Fitzpatrick, James E., and Woods, Robert L.: Low-Speed Lateral-Control Characteristics of an Unswept Wing With Hexagonal Airfoil Sections and Aspect Ratio 2.5 Equipped with Spoilers and With Sharp- and Thickened-Trailing-Edge Flap-Type Ailerons at a Reynolds Number of 7.6×10^6. NACA RM L52B15, 1952.

4. Fischel, Jack, and Hammond, Alexander, D.: Investigation of Effect of Span and Spanwise Location of Plain and Stepped Spoiler Ailerons on Lateral Control Characteristics of a Wing With Leading Edge Swept Back 51.3°. NACA RM L9K02, 1950.

5. Pasamanick, Jerome, and Sellers, Thomas B.: Low-Speed Investigation of the Effect of Several Flap and Spoiler Ailerons on the Lateral Characteristics of a 47.5° Sweptback-Wing-Fuselage Combination at a Reynolds Number of 4.4×10^6. NACA RM L50J20, 1950.

6. Vogler, Raymond D.: Wind-Tunnel Investigation at High Subsonic
    Speeds of Spoilers of Large Projection on an NACA 65A006 Wing With
    Quarter-Chord Line Swept Back 32.6°. NACA RM L51L10, 1952.

7. Fischel, Jack, and Hagerman, John R.: Effect of Aspect Ratio and
    Sweepback on the Low-Speed Lateral Control Characteristics of
    Untapered Low-Aspect-Ratio Wings Equipped with Retractable Ailerons.
    NACA TN 2347, 1951.

8. Hallissy, Joseph M., Jr., West, F. E., Jr., and Liner, George:
    Effects of Spoiler Ailerons on the Aerodynamic Load Distribution
    Over a 45° Sweptback Wing at Mach Numbers from 0.60 to 1.03.
    NACA RM L54C17a, 1954.

9. Fischel, Jack, and Tamburello, Vito: Investigation of Effect of
    Span, Spanwise Location, and Chordwise Location of Spoilers on
    Lateral Control Characteristics of a Tapered Wing. NACA TN 1294,
    1947.

10. Voepel, H.: German Wind Tunnel Tests on Trailing Edge Spoilers at
    Subsonic and Supersonic Speeds. British R.A.E. TN No. Aero 2214,
    British A.R.C., 1953.

11. Lowry, John G.: Data on Spoiler-Type Ailerons. NACA RM L53I24a,
    1953.

12. DeYoung, John: Theoretical Antisymmetric Span Loading for Wings of
    Arbitrary Plan Form at Subsonic Speeds. NACA Rep. 1056, 1951.
    (Supersedes NACA TN 2140)

TABLE I.- GEOMETRIC CHARACTERISTICS OF MODELS

Model	Configu-ration (λ)	A	$\Lambda_{c/4}$, deg	λ	Test conditions R, million	Test conditions M	Refer-ence	Airfoil section (streamwise unless otherwise indicated)	Spoiler spanwise extent $\eta_{i min}$	Spoiler spanwise extent $\eta_{o max}$
1	W	3.00	15.94	0.40	9.7	0.13	1	Modified diamond $\left(\frac{t_{max}}{c} = 0.042\right)$	0	1.00
2	W+B	3.00	40.60	.40	9.7	.13	1	[a]NACA 64A006 $\pm 0.31c$	.148	1.00
3	W+B+V	2.99	45.00	0	12.8	.13	1	NACA 0005 mod.	.148	1.00
4	W+B+V	4.78	35.00	.51	7.17	.13	1	Root: NACA 0012-64 Tip: NACA 0011-64 mod. $\pm 0.25c$	.10	1.00
5	W	4.01	40.18	.62	6.8	.16	2	NACA 64_1-112 $\pm 0.273c$	0	.98
6	W+B	2.5	5.28	.62	7.6	.15	3	Hexagonal $\left(\frac{t_{max}}{c} = 0.06\right)$	.20	.95
7	W	3.11	48.77	.50	1.3	.13	4	NACA 65_1-012	0	1.00
8	W+B	3.4	45.00	.51	4.4	.07	5	NACA 64_1-A112 $\pm 0.25c$	.12	.98
9	W+B	4.0	32.6	.60	2.0	.40 .60 .80	6	NACA 65A006	.139	.639
10	W	4.13	0	1.00	2.2	.26	7	NACA 64A010	.376	.976
11	W	2.13	0	1.00	3.1	.26	7	NACA 64A010	.352	.952
12	W	2.09	45.0	1.00	3.1	.26	7	NACA 64A010 $\pm 0.25c$	0	1.0
[a]13	W+B	3.98	45.0	.61	5	.60	8	NACA 65A006	.14	.87

[1]Configuration designations: W, wing; B, fuselage; V, vertical tail.
[2]This model was also tested with a section modified by the addition of a drooped leading edge of increased radius.
[3]It should be noted that the spoiler reported on in reference 8 was curved and, therefore, not entirely normal to the wing surface; however, since the deflection is measured normal to the wing surface and the curvature is small, these data are included in this report.
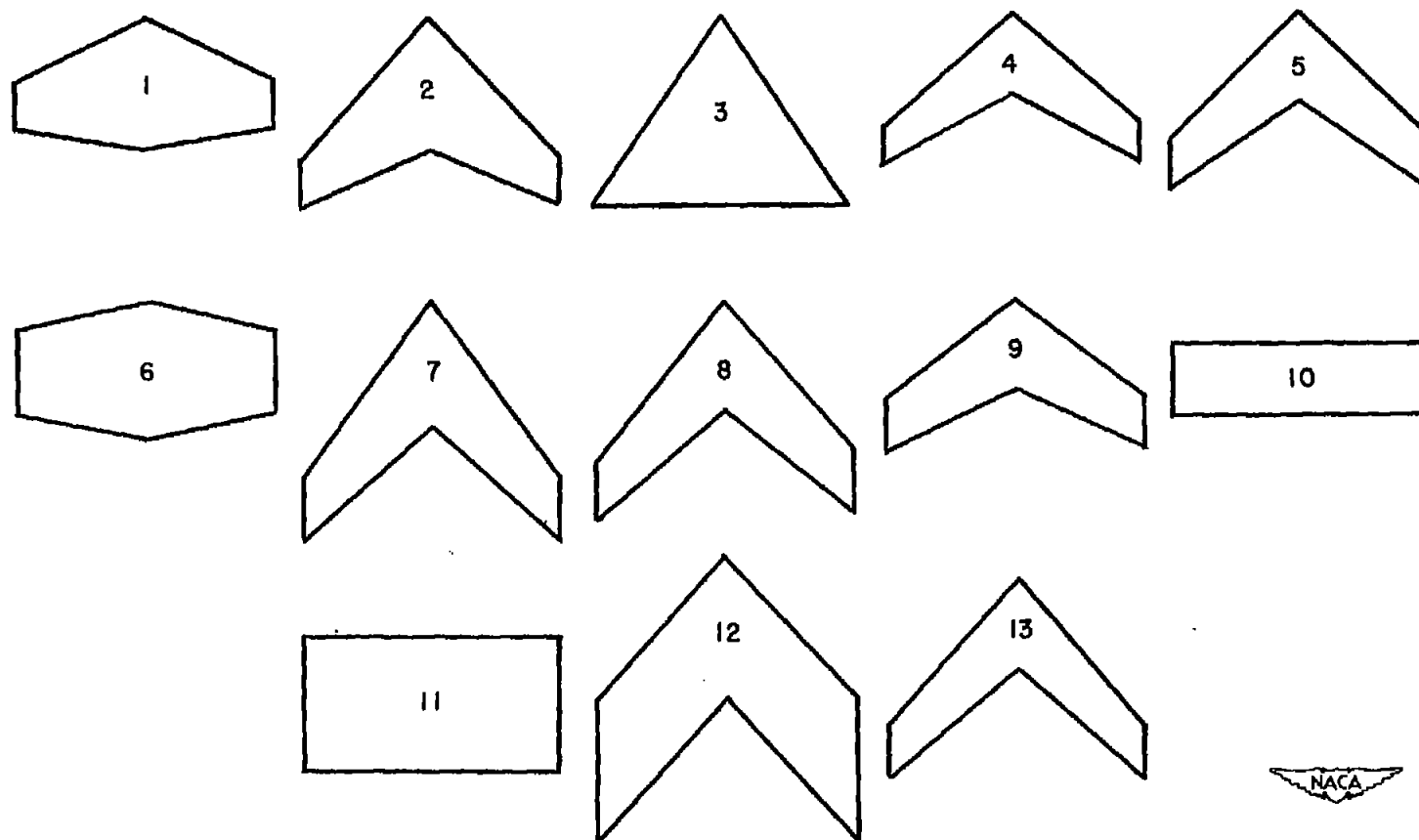
Figure 1.- Summary of wing plan forms of models. (Model numbers correspond to those used in table I.)
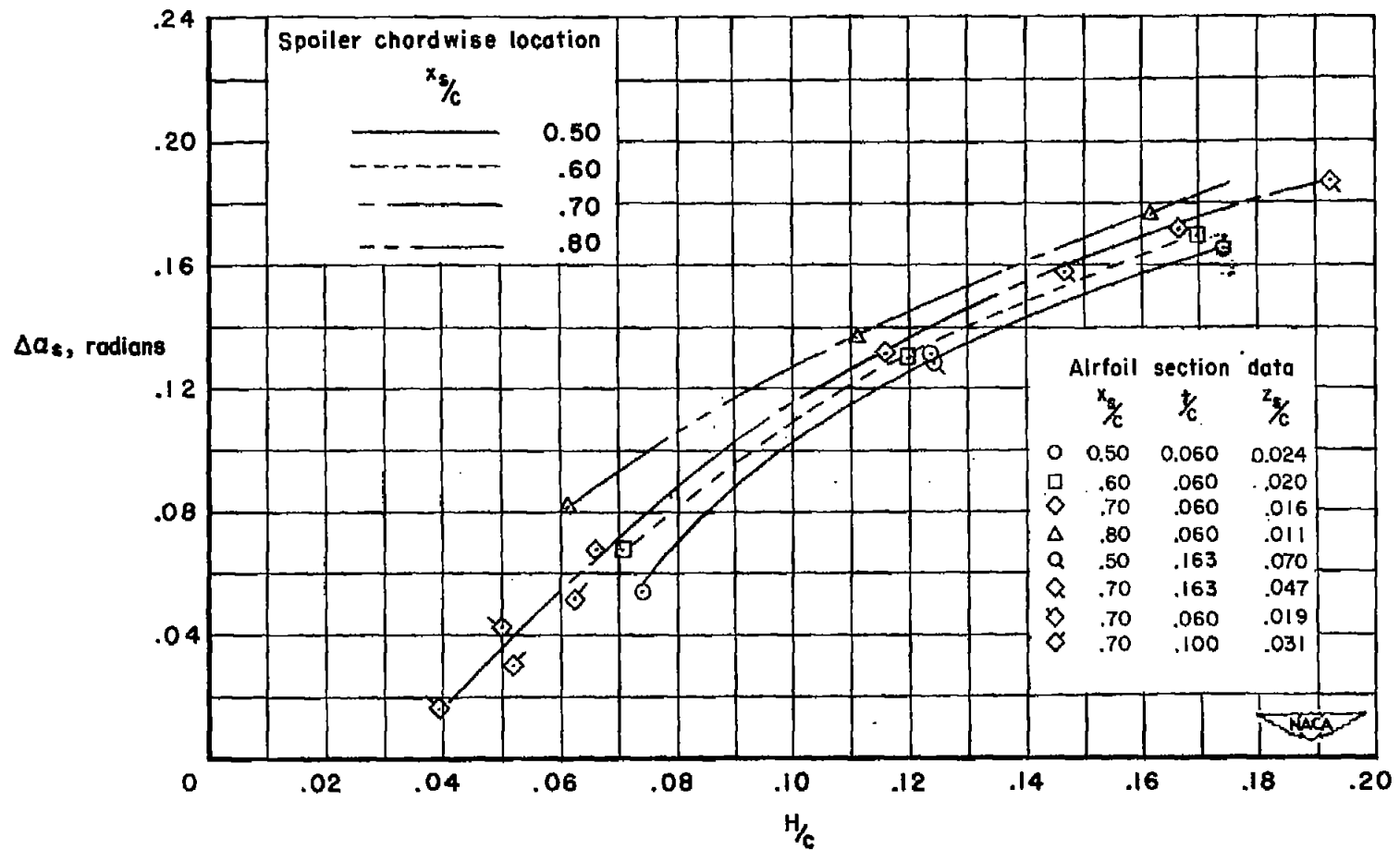
Figure 2.- Variation of $\Delta\alpha_s$ with effective spoiler height for four chordwise locations.
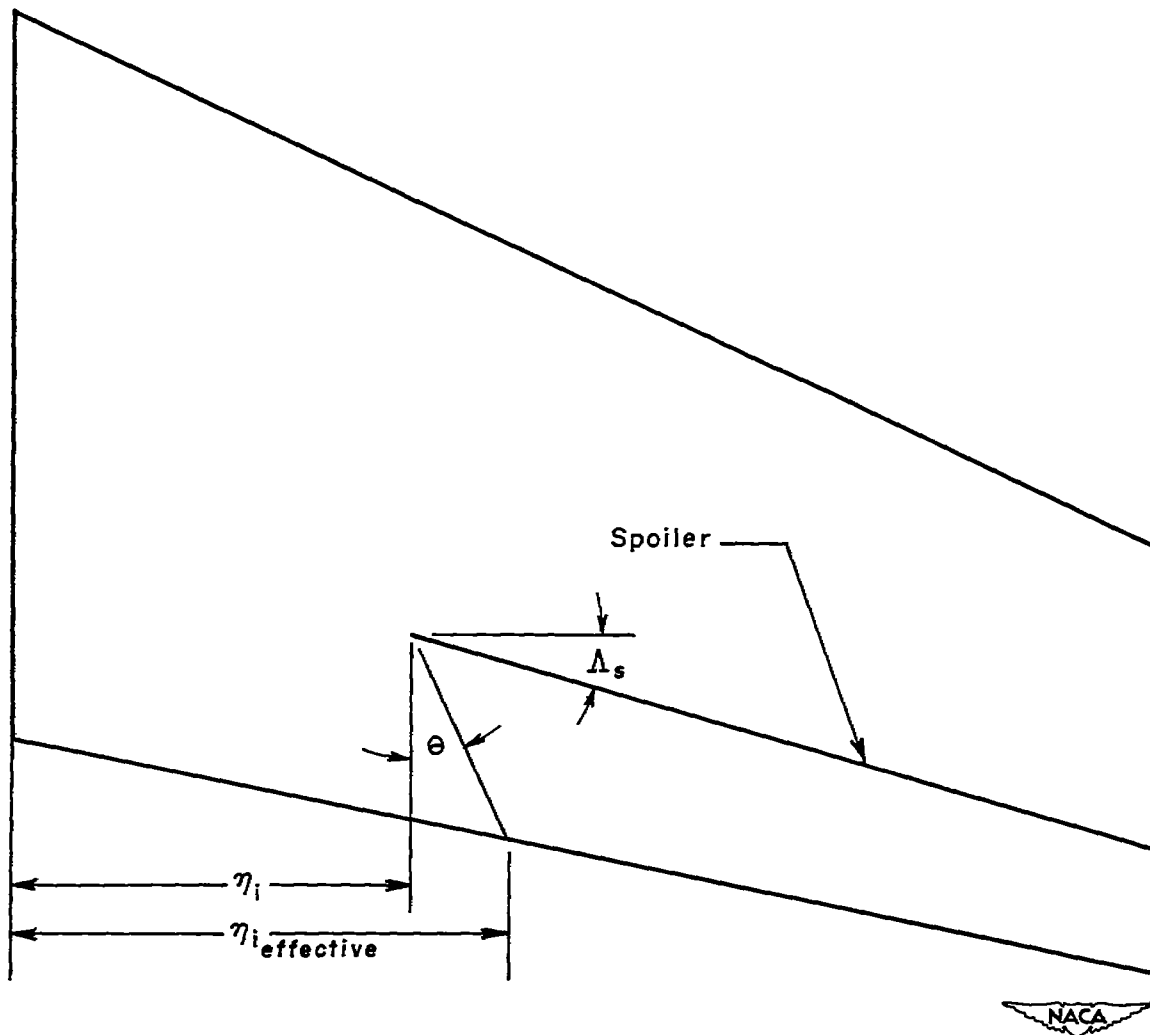
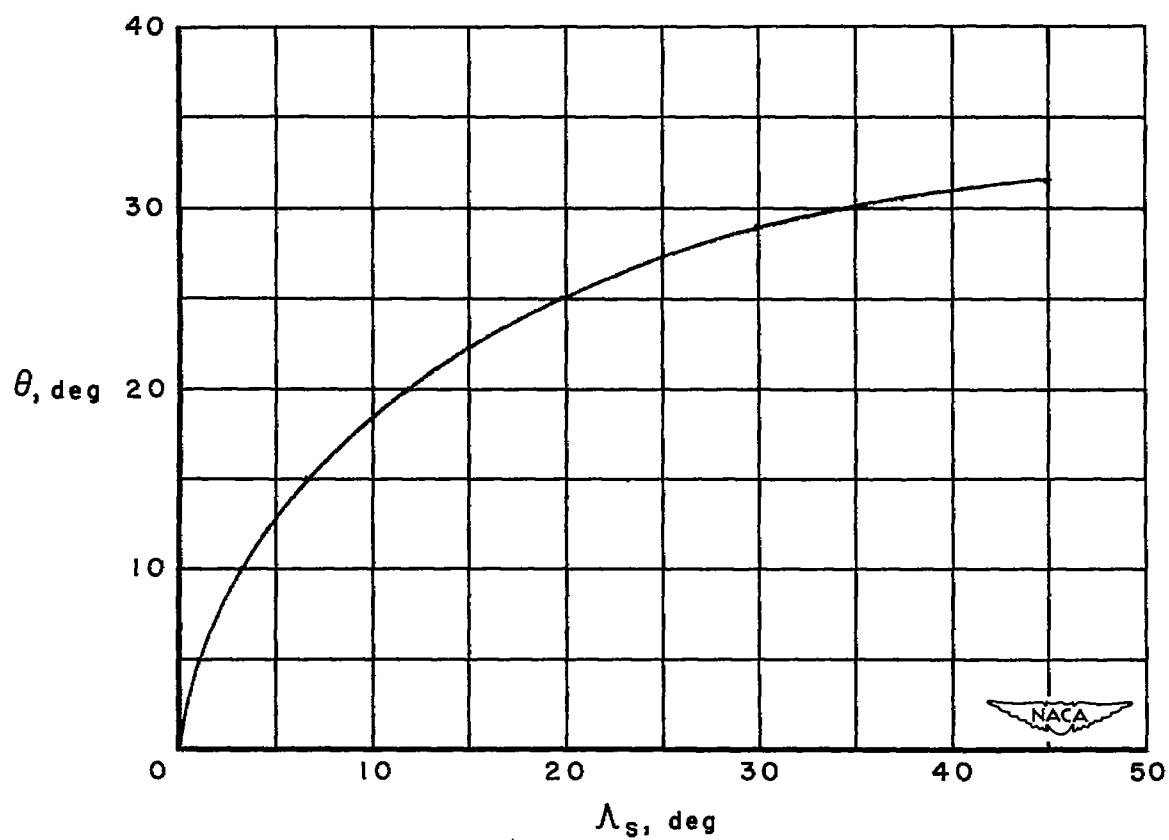Figure 3.- Determination of θ for a spoiler extending inboard from the tip.

Figure 4.- Variation of θ with angle of sweepback of spoiler at $\frac{x_s}{c} = 0.70$.

$$\eta_{i_{effective}} = \eta_i + \frac{4\left(1 - \frac{x_s}{c}\right)}{A(1+\lambda)}\left[1 - (1-\lambda)\eta_i\right]\frac{\cos\Lambda_T\sin\Theta}{\cos(\Lambda_T+\Theta)}$$

$$\eta_{o_{effective}} = \eta_o + \frac{4\left(1 - \frac{x_s}{c}\right)}{A(1+\lambda)}\left[1 - (1-\lambda)\eta_o\right]\frac{\cos\Lambda_T\sin\Theta}{\cos(\Lambda_T+\Theta)}$$
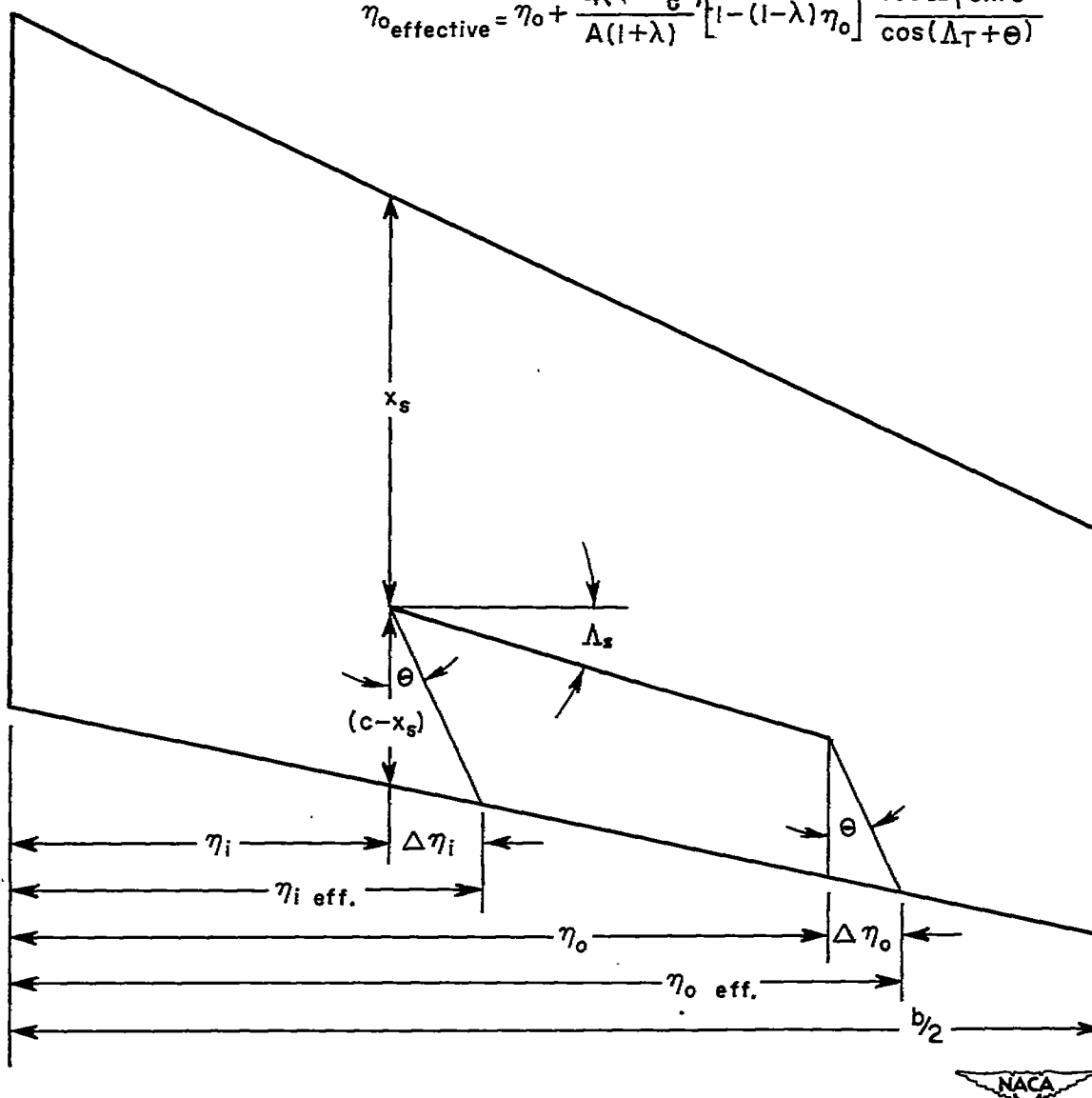
Figure 5.- Method of determining effective spanwise extent of an arbitrarily located spoiler aileron.

(a) $h/c = 0.05$

(b) $h/c = 0.10$

(c) $h/c = 0.15$

	η_i	η_o
○	0	0.2
□		0.4
△		0.6
◇		0.8
◺		1.0
◓	0.8	1.0
◔	0.6	
◭	0.4	
◈	0.2	
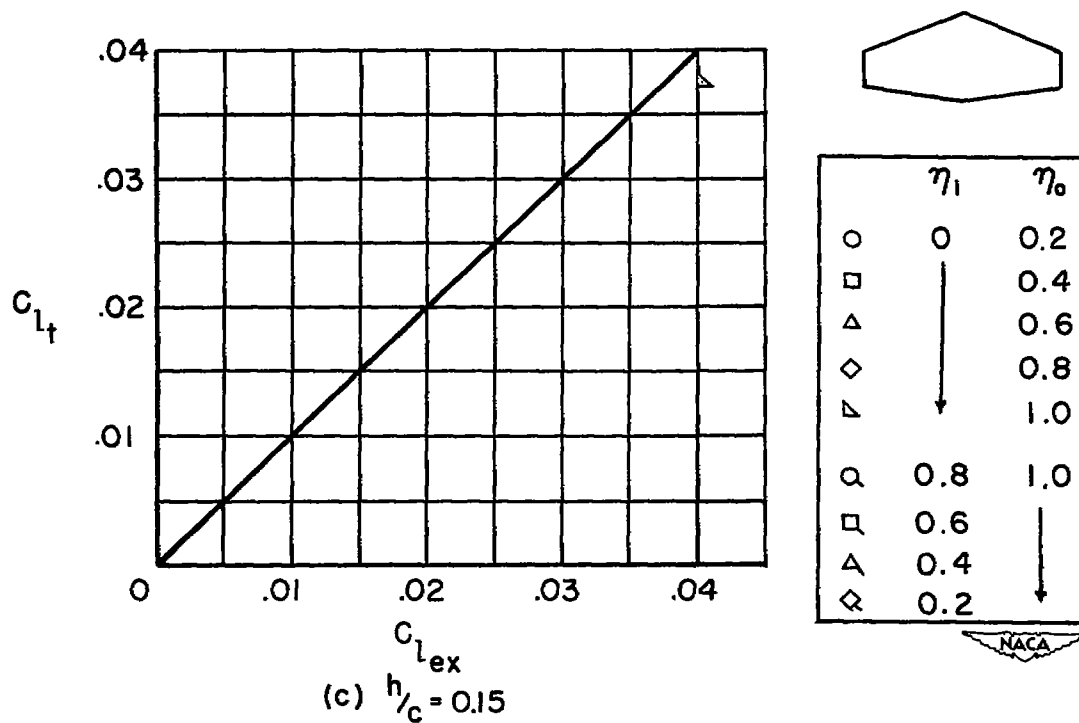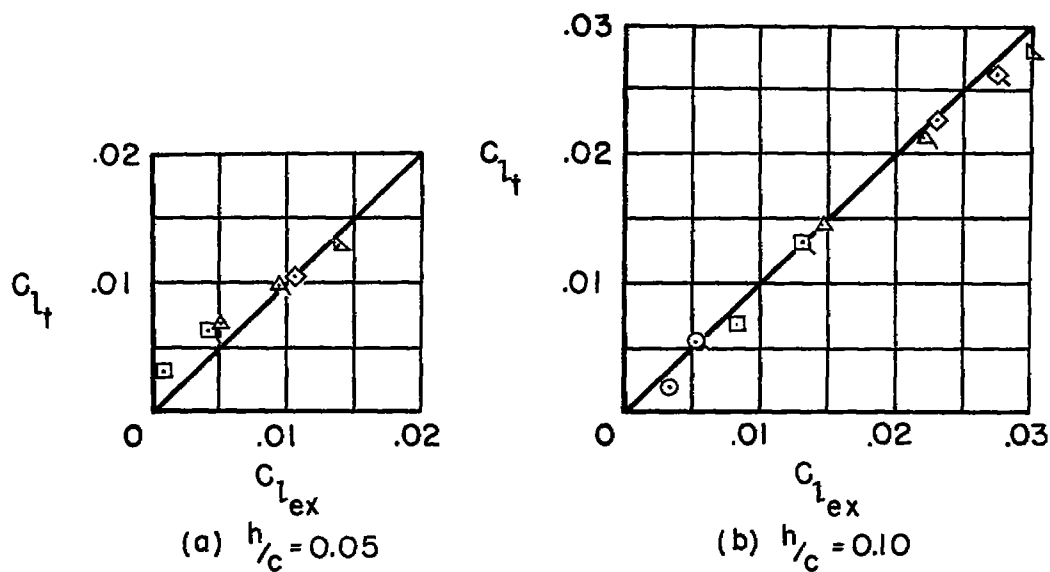
Figure 6.- Experimental and predicted rolling-moment coefficients for model 1; $\frac{x_s}{c} = 0.70$.

C_{1_t} .01

.02

.01

0   .01   .02

$C_{1_{ex}}$

(a) $h/c = 0.05$

.03

C_{1_t}

.02

.01

0   .01   .02   .03

$C_{1_{ex}}$
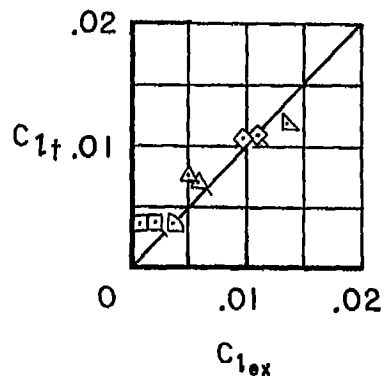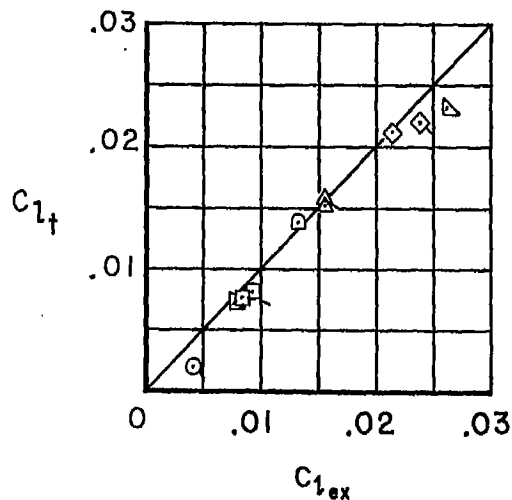
(b) $h/c = 0.10$

	η_i	η_o
○	0.15	0.2
□		0.4
△		0.6
◇		0.8
◁		1.0
◁	0.4	0.6
◠	0.2	0.6
◔	0.8	1.0
◷	0.6	
△	0.4	
◇	0.2	

.04

C_{1_t} .02

.03

.02

.01

0   .01   .02   .03   .04

$C_{1_{ex}}$
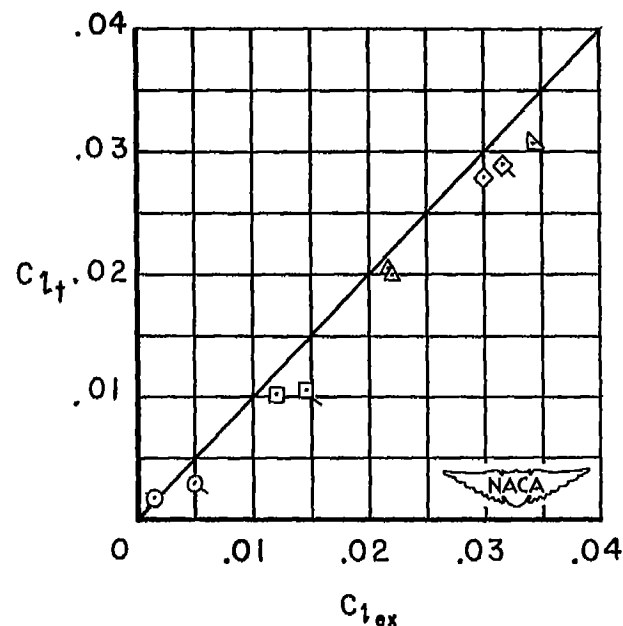
(c) $h/c = 0.15$

NACA

Figure 7.- Experimental and predicted rolling-moment coefficients for model 2; $\frac{x_s}{c} = 0.70$.
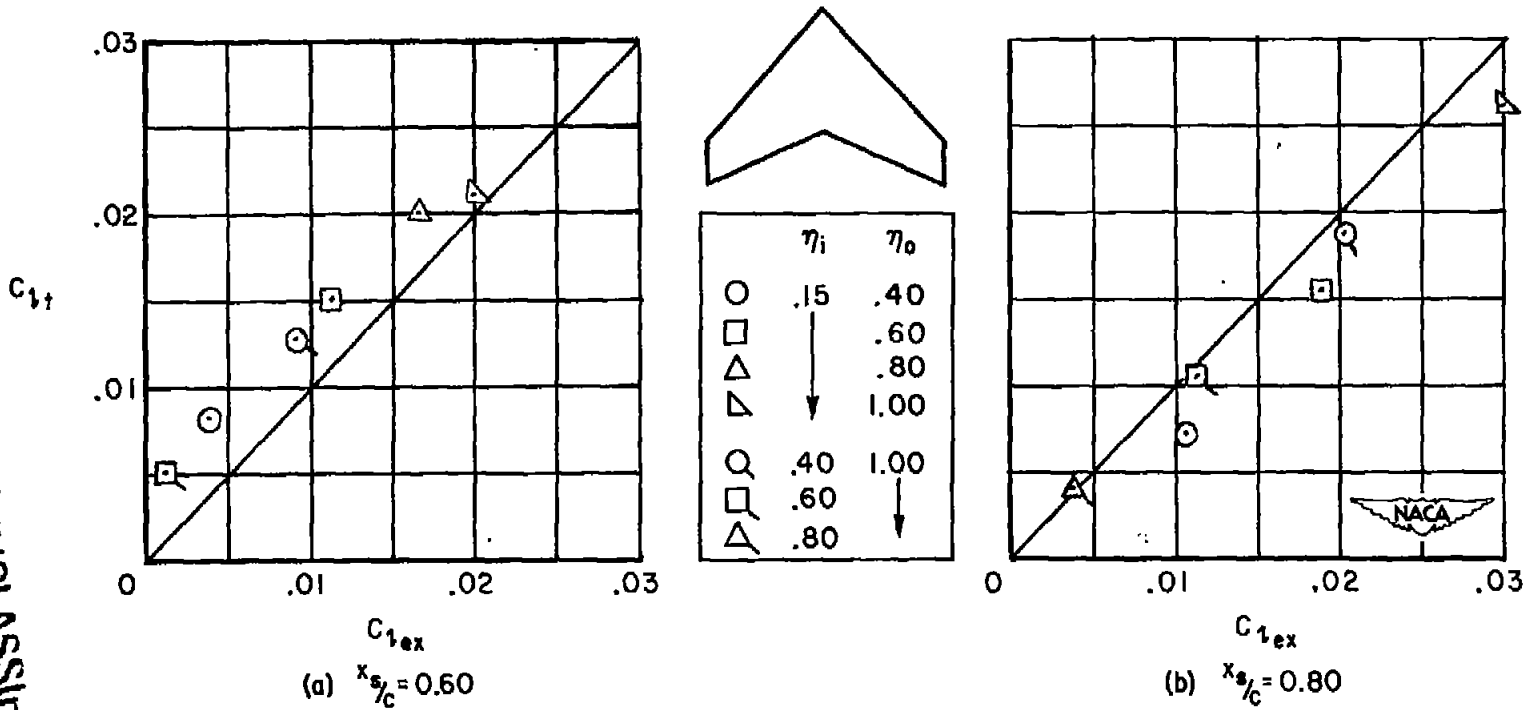
Figure 8.- Experimental and predicted rolling-moment coefficients for model 2; $\frac{h}{c} = 0.10$.
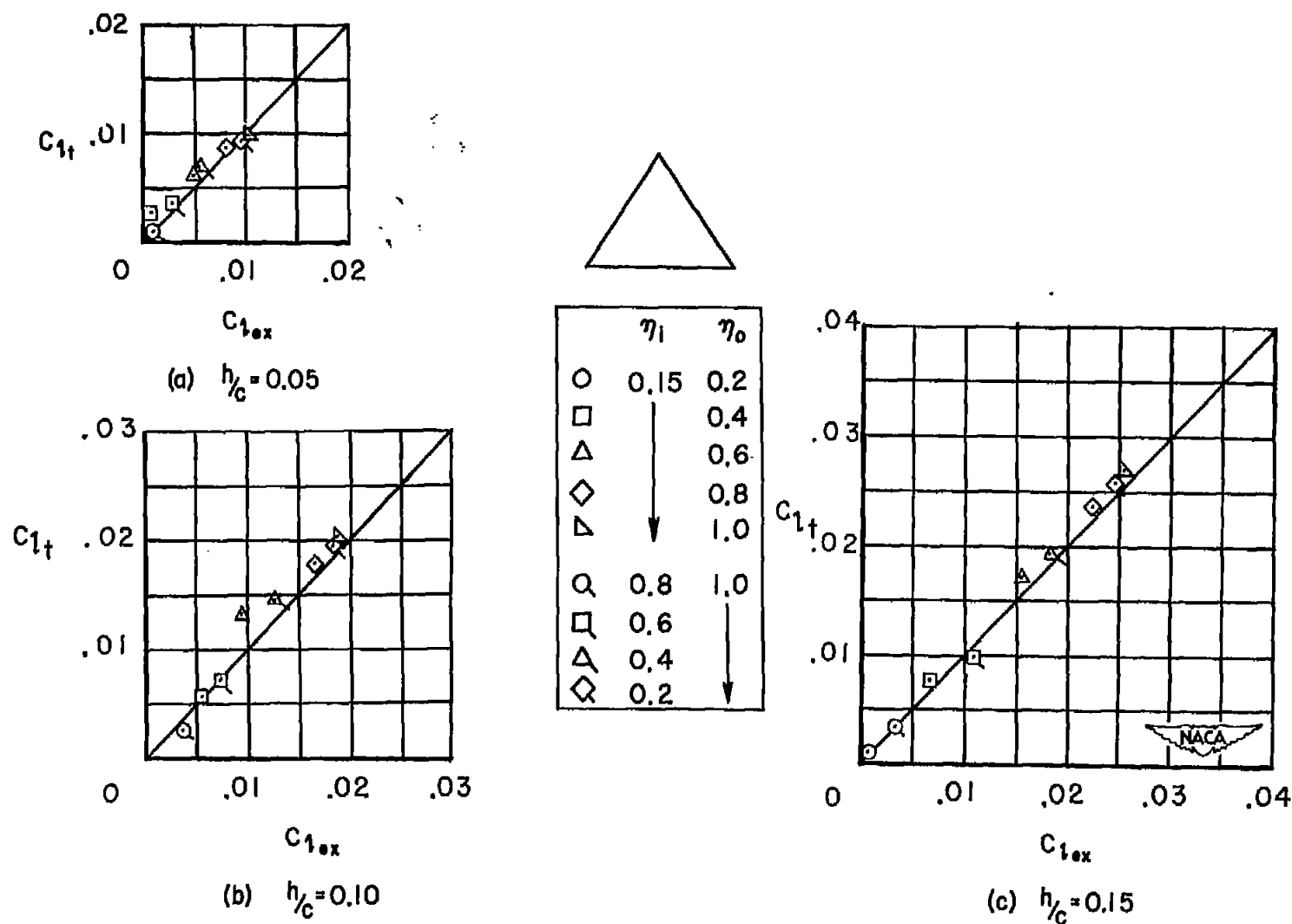
Figure 9.- Experimental and predicted rolling-moment coefficients for model 3; $\frac{x_s}{c} = 0.70$.

UNCLASSIFIED

(a) $h/c = .05$

(b) $h/c = .10$
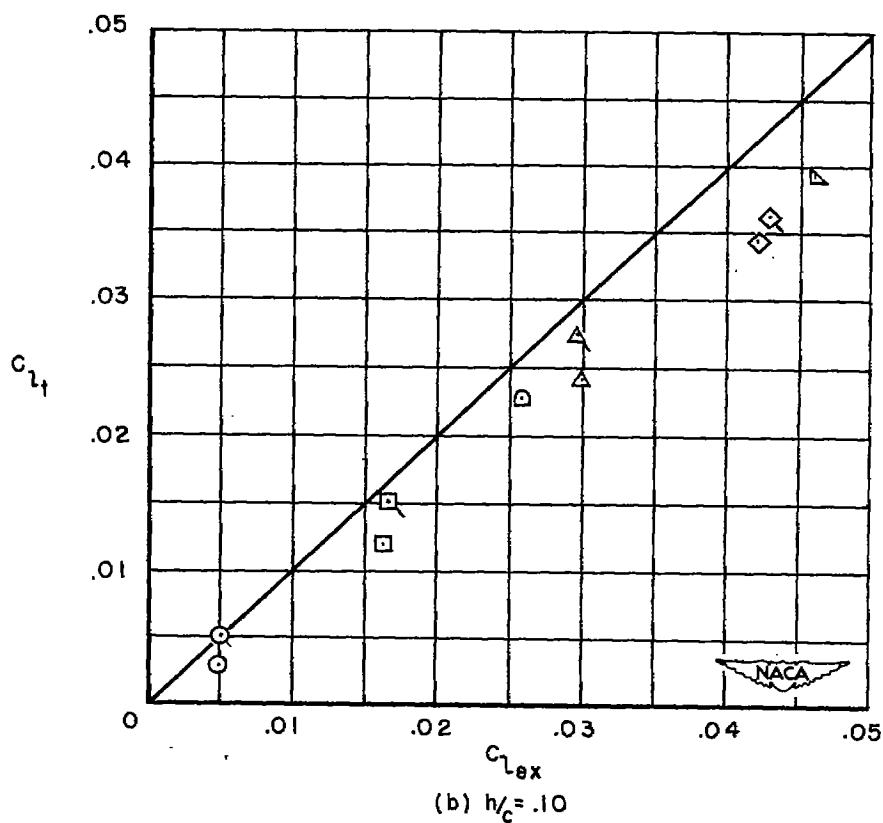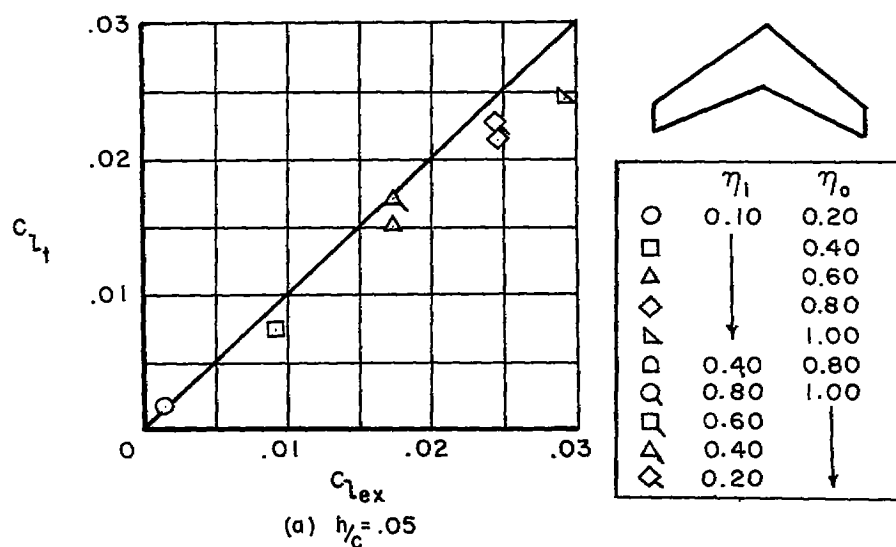
Figure 10.- Experimental and predicted rolling-moment coefficients for model 4; $\frac{x_g}{c} = 0.70$.

	η_1	η_0
○	0	0.4
□		0.6
△		0.8
◇		0.975
Q	0.8	0.975
⊡	0.6	
△	0.4	
◇	0.2	

(a) $h/c = 0.05$

(b) $h/c = 0.10$
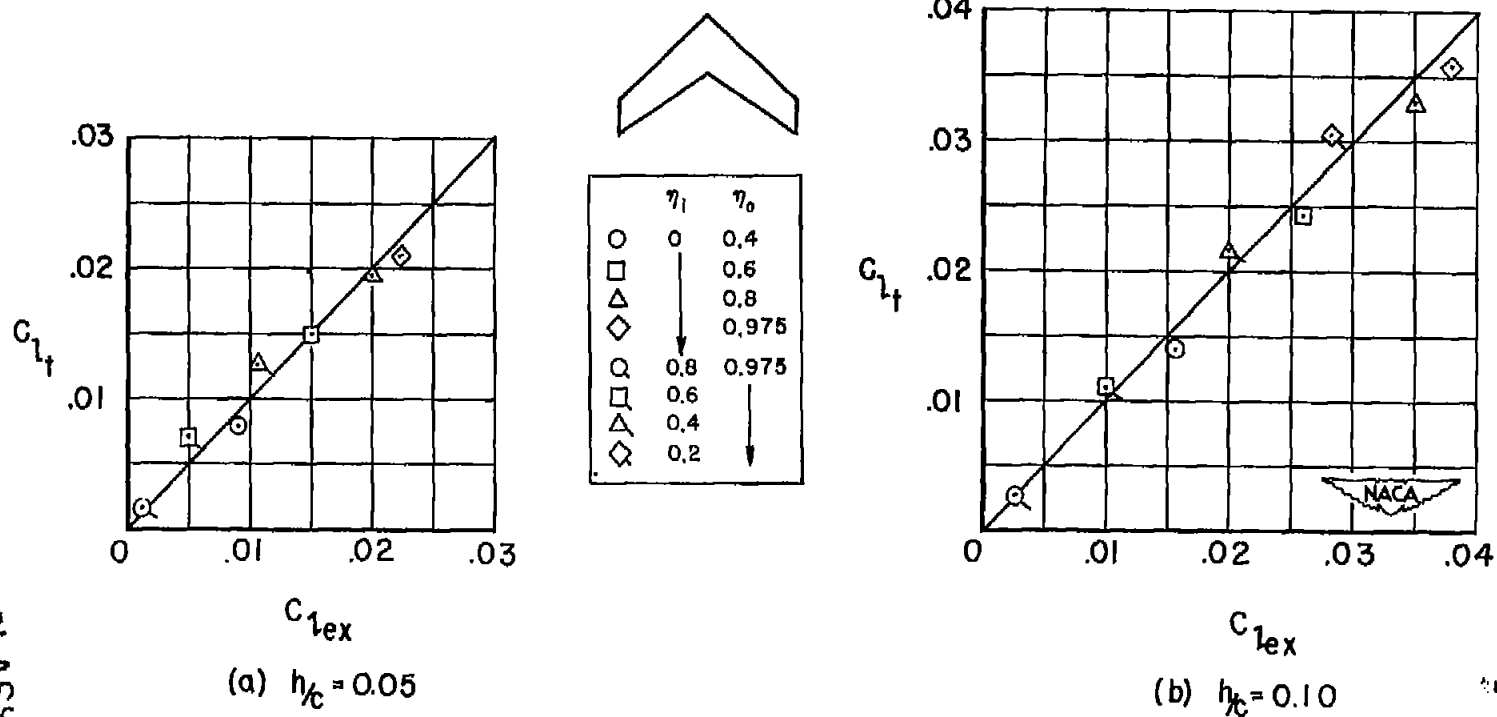
Figure 11.- Experimental and predicted rolling-moment coefficients for model 5; $\dfrac{x_s}{c} = 0.70$.
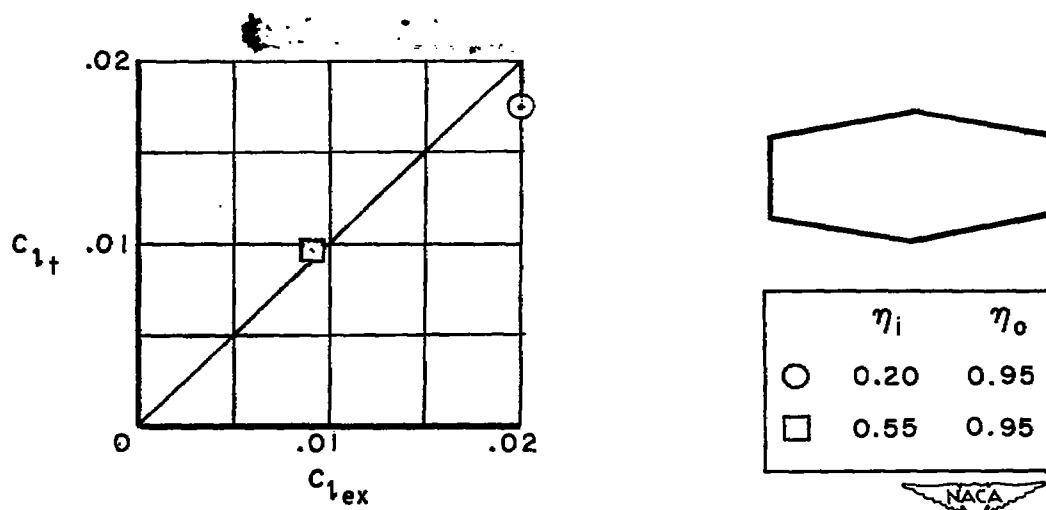
Figure 12.- Experimental and predicted rolling-moment coefficients for model 6; $\frac{x_s}{c} = 0.70$; $\frac{h}{c} = 0.06$.
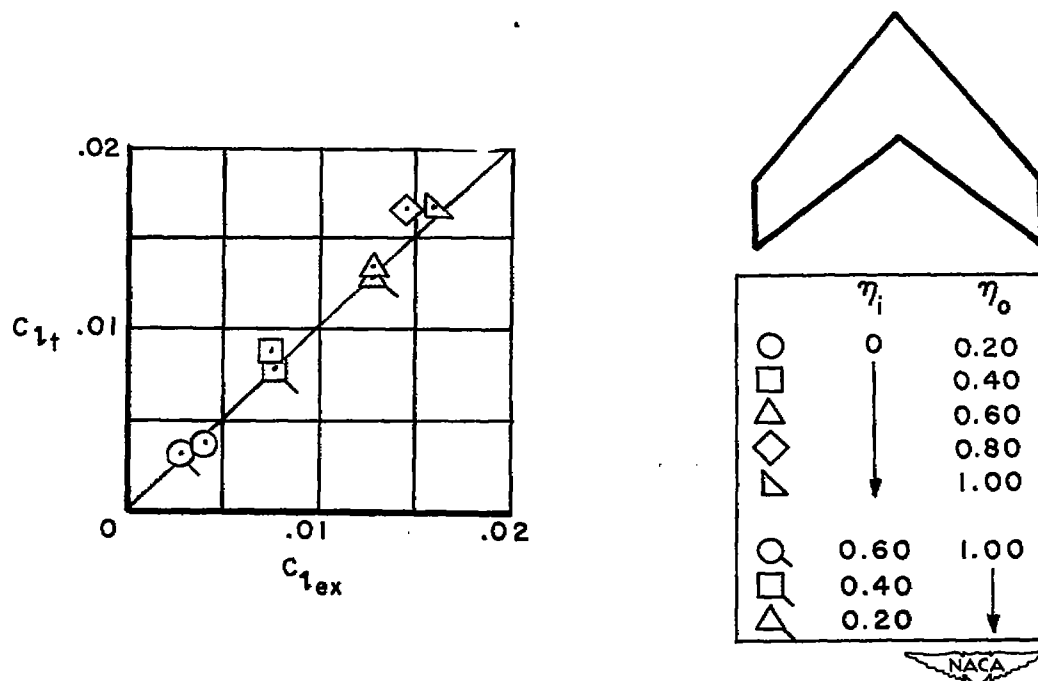
Figure 13.- Experimental and predicted rolling-moment coefficients for model 7; $\frac{x_s}{c} = 0.70$; $\frac{h}{c} = 0.05$.

	η_i	η_0
○	0.12	0.42
□		0.62
△	↓	0.82
◁		0.975
○	0.775	0.975
□	0.575	
△	0.375	
◁	0.175	↓

(a) $h/c = 0.05$

(b) $h/c = 0.10$
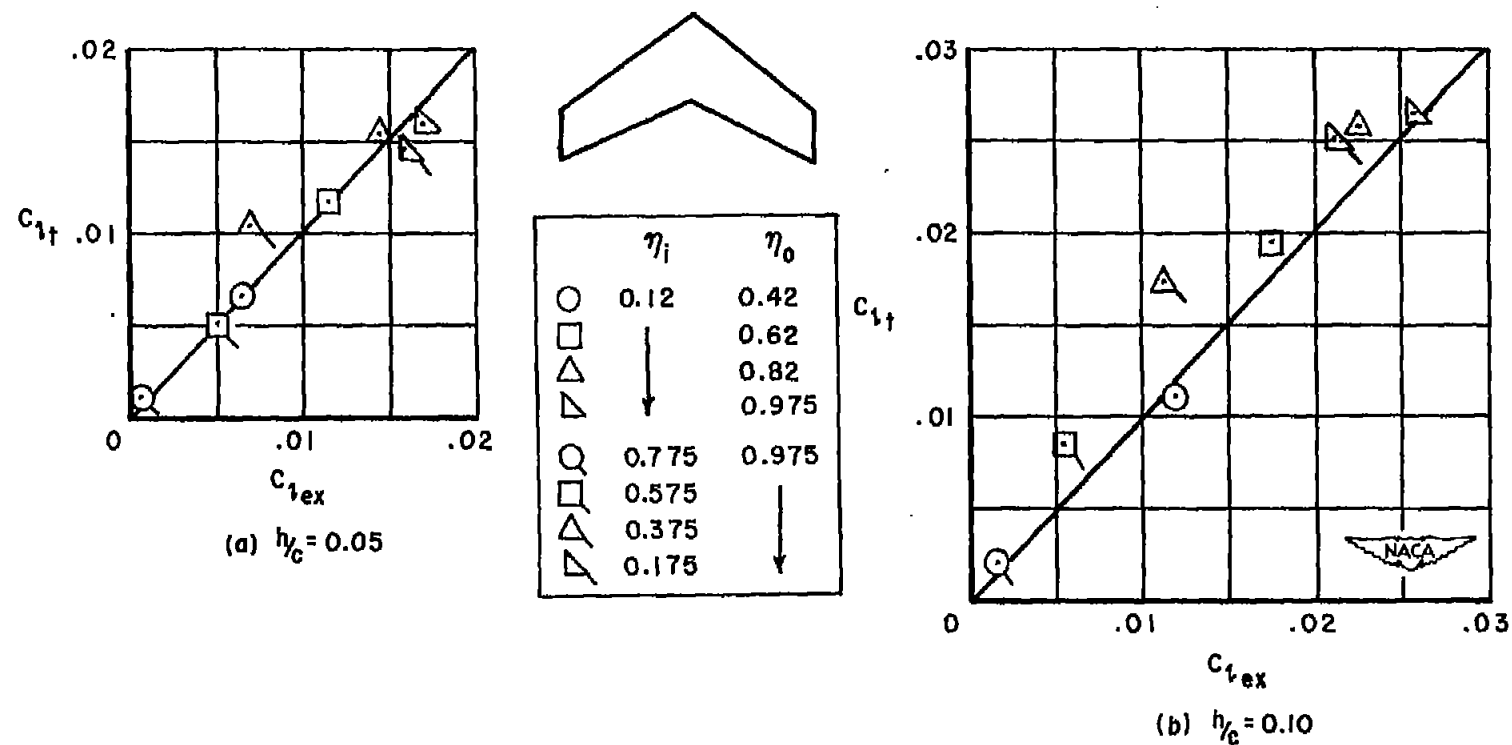
Figure 14.- Experimental and predicted rolling-moment coefficients for model 8; $\frac{x_B}{c} = 0.70$.
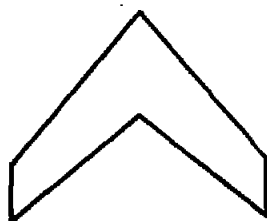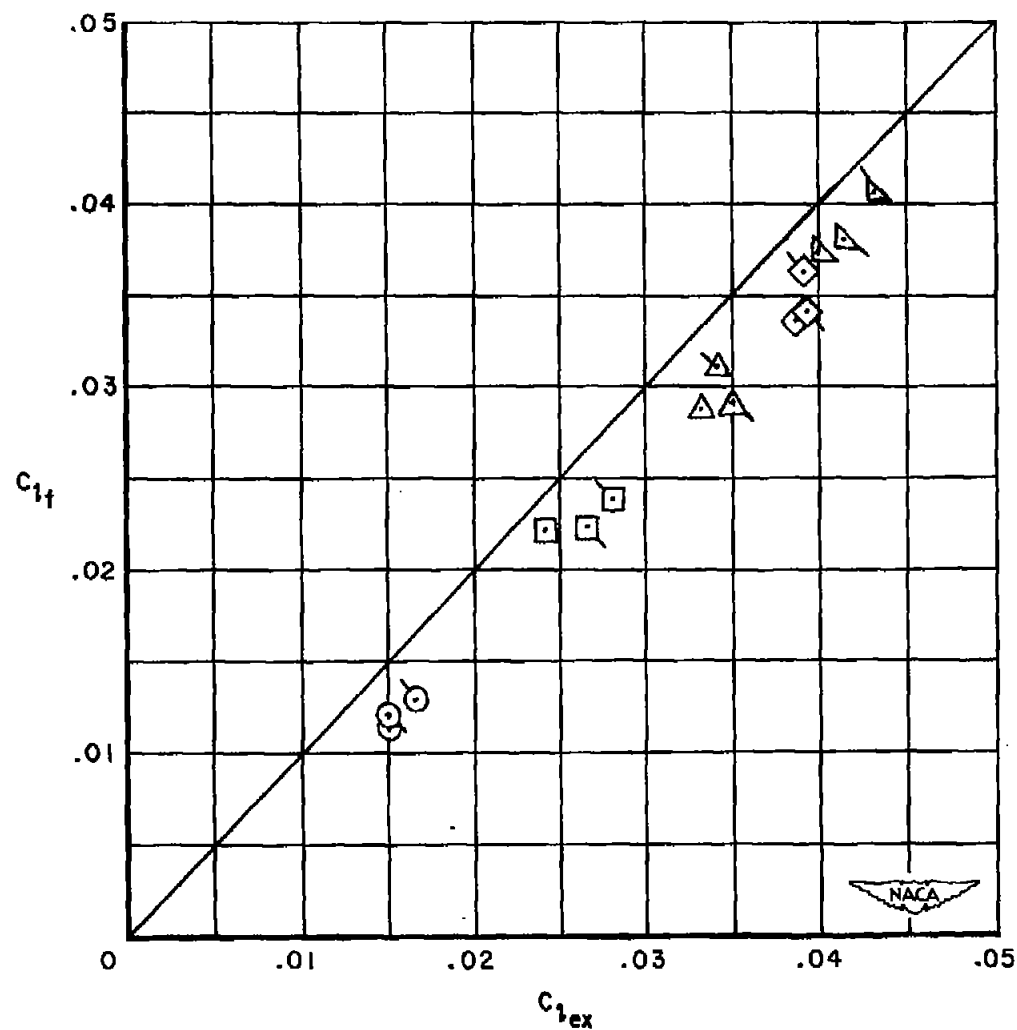
Figure 15.— Experimental and predicted rolling-moment coefficients for model 9; $\frac{x_s}{c} = 0.70$; $\eta_i = 0.139$; $\eta_o = 0.639$.
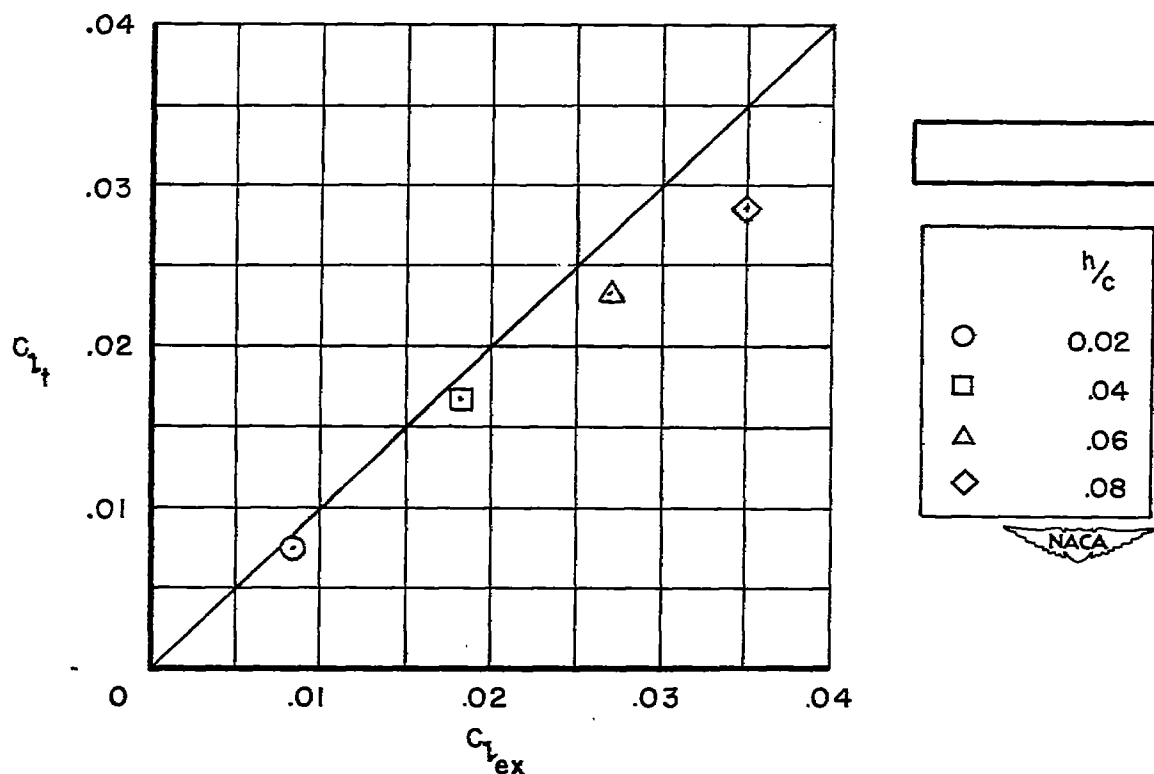
Figure 16.- Experimental and predicted rolling-moment coefficients for model 10; $\frac{x_B}{c} = 0.70$; $\eta_i = 0.34$; $\eta_o = 0.94$.

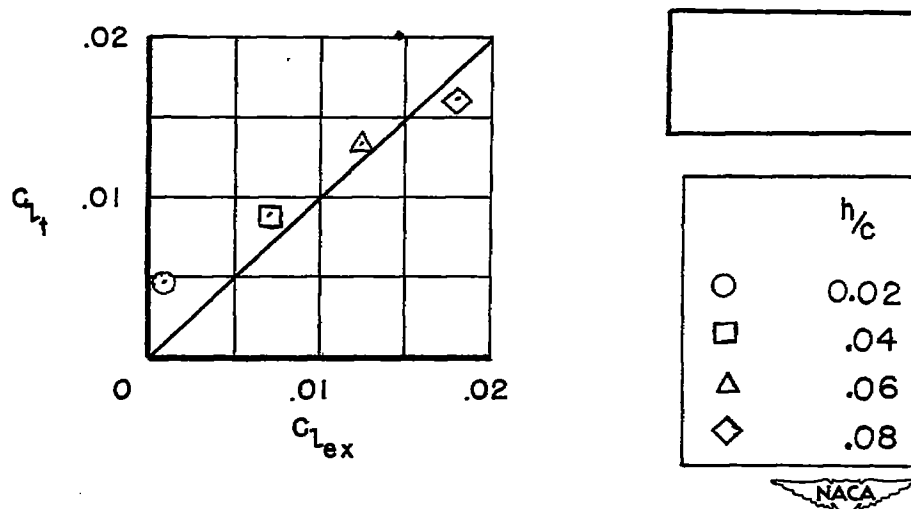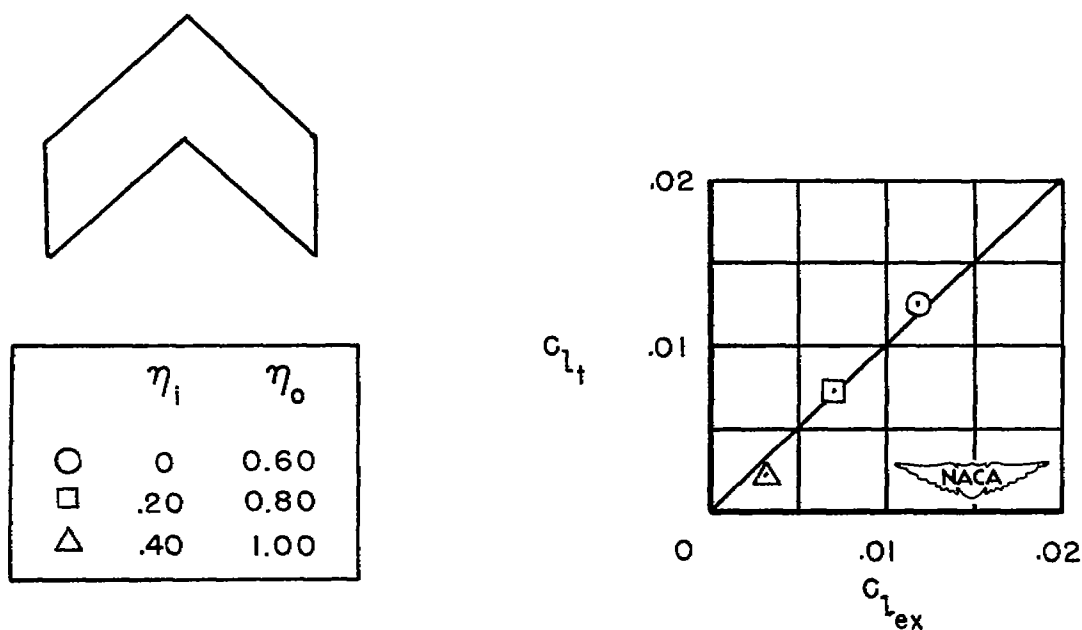Figure 17.- Experimental and predicted rolling-moment coefficients for model 11; $\frac{x_B}{c} = 0.70$; $\eta_i = 0.31$; $\eta_o = 0.91$.

Figure 18.- Experimental and predicted rolling-moment coefficients for model 12; $\frac{x_s}{c} = 0.70$; $\frac{h}{c} = 0.08$.

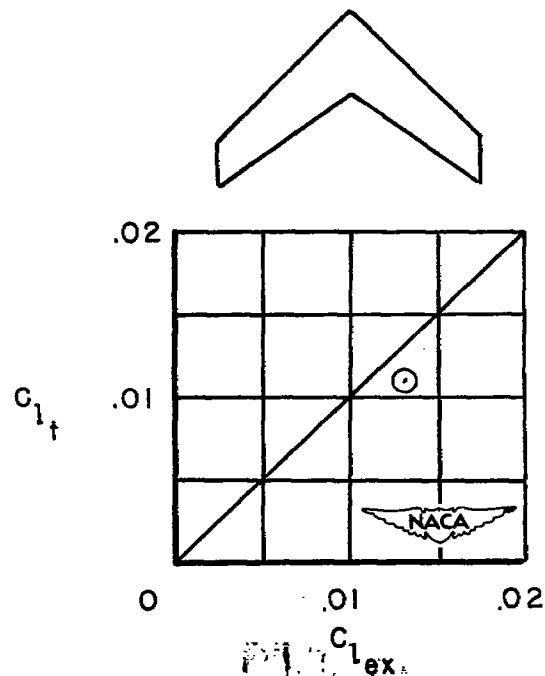
Figure 19.- Experimental and predicted rolling-moment coefficients for model 13; $\frac{x_s}{c} = 0.70$; $\frac{h}{c} = 0.04$; $\eta_i = 0.14$; $\eta_o = 0.87$.
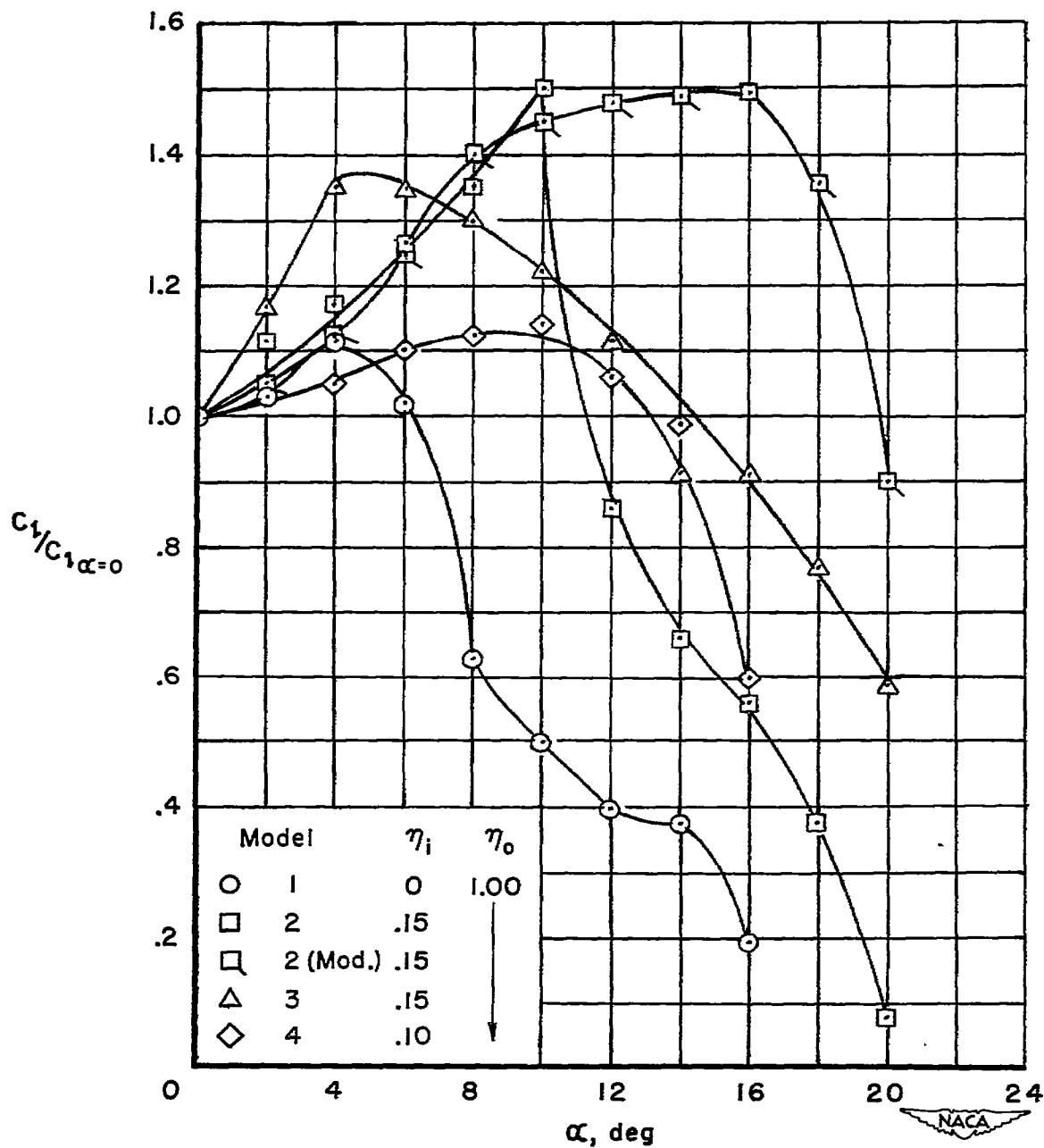
Figure 20.- The ratio of rolling-moment coefficient at various angles of attack to the rolling-moment coefficient at zero angle of attack; $\frac{h}{c} = 0.10$; $\frac{x_s}{c} = 0.70$.